Plasmonics (2015) 10:1687–1693
DOI 10.1007/s11468-015-9989-z

Tunable Fano Resonances and Electromagnetically Induced Transparency in All-Dielectric Holey Block

Naseer Muhammad[1] · **Adnan Daud Khan**[1]

Received: 4 March 2015 / Accepted: 20 May 2015 / Published online: 28 May 2015

Abstract The optical properties of a simple planar silicon nanoblock with cylindrical hole operating at terahertz (THz) frequencies are investigated. The proposed nanostructure exhibit low loss electromagnetically induced transparency (EIT) and Fano resonances, which arises due to the near-field coupling between the nanoblock and cavity modes. The line shape of these resonances can be considerably modified and tuned by varying the geometrical parameters. Furthermore, the symmetry breaking conception is also introduced, which enables higher-order dark hybridized modes to interact with each other, resulting in a dual EIT and Fano resonances in the optical spectrum. The EIT and Fano resonances present high local field enhancement (33) and Q-factors (584) due to extremely low absorption loss. This makes the proposed design an ideal platform for low loss slow-light devices and multi-wavelength biosensing applications.

Keywords Dielectric nanostructures · Symmetry breaking · EIT · Fano resonance · Q-factor

Introduction

A rapidly expanding militia of electromagnetically induced transparency (EIT) and Fano resonances in all-dielectric high refractive index materials has taken the planet of nanosystems by storm. All-dielectric materials offer best solution and a new route to the bottlenecks of metallic nanosystems including Q-factor and field enhancement. Electromagnetically induced transparency is a concept initially examined in atomic systems, which usually arises due to quantum destructive interference resulting in a narrow band highly dispersive transparency window for light propagating through an originally opaque medium [1]. Later on, this theory was extended to plasmonic nanostructures [2–8].

In plasmonic nanosystems, EIT and Fano resonances usually originate from the destructive interference of a narrow band and broad band spectra, which results in a sharp asymmetric line shape [9–18]. The line shape of such resonances is highly sensitive to the local dielectric medium and geometry of the nanoparticle. These resonances become popular in recent years due to sharp spectral features, which can be used for the development of chemical or biological sensors, lasing, and slow-light devices [19]. Several plasmonic nanostructures are proposed by different research groups to study the effect of EIT and Fano resonances, which include nanodisks [20], nanoshells [11, 21], nanodimers [22, 23], nanotrimers [24], and nanoparticle aggregates [25, 26]. In all these nanostructures, the plasmon modes of the individual nanoparticles can interact and produce EIT and Fano resonances [11, 12]. For multi-wavelength biosensor and plasmon line shaping applications, multiple or higher-order EIT and Fano resonances are required. The most efficient way of achieving multiple EIT and Fano resonances in metal nanostructures is symmetry breaking, which allows access to different resonant modes that are not readily accessible in symmetric configurations [10, 13, 27–29].

The main limitation of the plasmonic nanosystems is the large ohmic losses, which limits the Q-factor to <~10. So, absorption in metal nanoparticles decreases the efficiency of

✉ Adnan Daud Khan
adnandaudkhan@gmail.com

Naseer Muhammad
engr_naseermuhd@hotmail.com

[1] Department of Electrical Engineering, Sarhad University of Science & Information Technology, Landi Akhun Ahmad, Ring Road, 25000 Peshawar, Pakistan

the EIT and Fano resonances. To reduce the losses, researchers have reported that the use of silicon-based dielectric nanostructures like oligomers [30–32] and nanorod arrays [33] produces EIT and Fano resonances with large Q-factors that reach to several hundreds or even higher [34, 35]. Therefore, the use of high refractive index dielectric nanostructures is a perfect option to produce EIT and Fano resonances with high Q-factors, which make them promising for low loss slow-light devices and biosensing applications.

In this article, we present the observation of low loss EIT and Fano resonances in a simple periodic array of square silicon block with a cylindrical hole. The proposed nanostructure exhibits EIT and Fano resonances, which arises due to interference of solid silicon block modes and cavity modes. These resonances can be tuned and enhanced in the optical spectrum by modifying the geometrical parameters of the proposed design. The symmetry breaking concept is also initiated in the silicon holey block, and multiple sharp EIT and Fano resonances are achieved in the optical spectrum. Such multiple EIT and Fano resonances supported by our proposed design have never been reported before in any dielectric nanostructure. Moreover, the extremely high-quality factors and field enhancement calculated at EIT and Fano resonances offer an effective platform for low loss slow-light devices and biosensors.

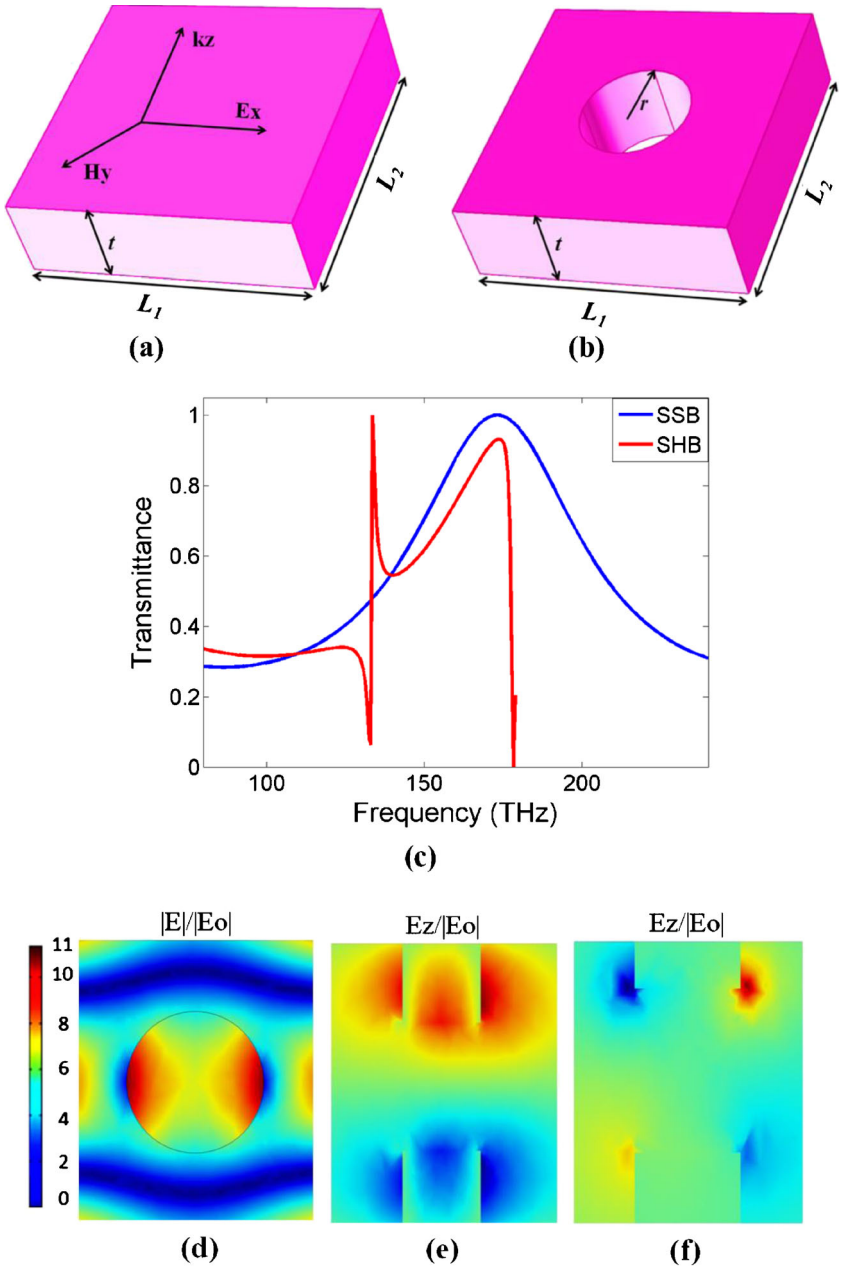

Fig. 1 Schematic of **a** solid silicon square block, and **b** silicon holey block (SHB) nanostructure. The geometrical parameters are t=250 nm, r=200 nm, and L_1=L_2=1000 nm, respectively. **c** Simulated transmittance spectra of solid silicon block (*blue curve*), and silicon holey block nanostructure (*red curve*). **d** Normalized electric field distribution at Fano resonance (*xy*-plane). **e** Electric field in the *z*-direction normalized to the field amplitude (E_0) of the incident light (*zx*-plane)

Geometry and Simulation Method

The schematic geometry of a silicon holey block (SHB) is illustrated in Fig. 1a, b. The structure is created from a periodic lattice composed of silicon square block with an air hole. The thickness of the SHB is t, and the radius of the cylindrical hole is r. Throughout the paper, the lengths L_1 and L_2 are made equal, and their values are fixed at 1000 nm. The period of the square unit cell is 1000 nm. The plane wave is normally incident on SHB structure, and the electric field is polarized along the x-axis. All the calculations are carried out in COMSOL Multiphysics software. The silicon is assumed to be lossless, with a refractive index of n=3.46 [34, 35], and the embedding medium is considered air for all the simulations.

Results and Discussion

Figure 1c shows the numerically calculated transmittance characteristics of the solid silicon block (SSB) without hole (blue curve) and SHB nanostructure (red curve). The thicknesses of both the nanostructures are fixed at 250 nm. The blue curve represents the fundamental broad dipole resonant mode around 175 THz, which is efficiently excited by incident light. By the introduction of cylindrical hole in the square block (SHB) with radius of 200 nm (Fig. 1b), the solid block and cavity modes hybridized and excite a narrow mode around 132 THz. This mode was originally dark in the SSB nanostructure and is typically representing a quadrupole mode as shown by the polarization charge distribution in Fig. 1e (zx-plane), where the red spot represents positive and blue spot represents negative. The coherent coupling and interference of the broad dipole and narrow quadrupole mode lead to Fano resonance with sharp asymmetric line shape in the optical spectrum. The dipole mode in SHB nanostructure almost sustains its position, while its spectral features slightly narrowed because of hybridization with cavity modes. Due to extremely small absorption loss, the calculated Q-factor at Fano resonance is about 147, and the peak transmission is near unity. This determines the potential to realize extremely dispersive and lossless, slow-light devices [34].

Figure 1d describes the electric field distribution of SHB nanostructure at Fano resonance in the xy-plane. The electric field is confined in the cavity similar like plasmonic nanostructures, and the highest value of the field enhancement achieved is 11, which is higher than the broad dipole mode's

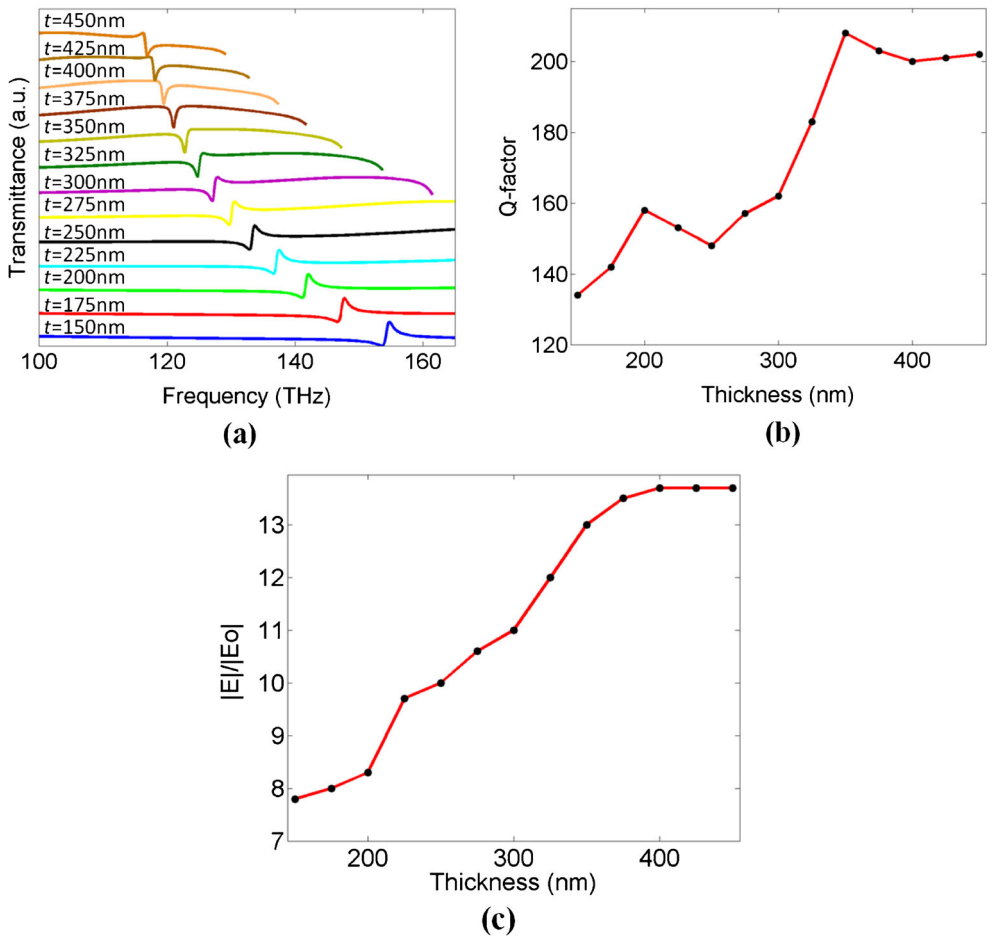

Fig. 2 **a** Transmittance spectra of silicon holey block (SHB) nanostructure for different thickness values at fixed hole radius r= 200 nm. **b** Extracted Q-factors versus the thickness t. **c** Dependence of the maximum field enhancement on thickness t

enhancement value (2). So, the proposed design is also suitable for biosensing application [35].

Tunability of Fano Resonance

In this section, we investigate the tunability of Fano resonance by changing the geometrical parameters of SHB nanostructure. First, we fixed the radius r=200 nm, and varied the thickness t of the SHB nanostructure. Figure 2a revealed the calculated transmittance spectra for different values of t. A large red shift of the Fano resonance from 155 to 117 THz is observed by increasing the thickness of the SHB from 150 to 450 nm. Along with the spectral position, the sharp asymmetric line shape of the Fano resonance also changes significantly by modifying t. For instance, at t=350 nm, a sharp dip appears between the dipole and quadrupole modes, which is the characteristic feature of EIT. Extreme dispersion is created in the EIT window, which can create slow light. By further increasing the value of t, the dip of EIT decreases. Figure 2b shows the Q-factor against various thickness values. The Q-factor increases by increasing t from 150 to 200 nm and then slightly drops at t=250 nm. By further increasing t, the Q-factor grows again significantly and the value reaches above 200 at t=350 nm. At t=375 nm, it drops to 200 and then remain almost smooth up to t=450 nm. Thus, the SHB nanostructure offers high values of the Q-factor at different t,

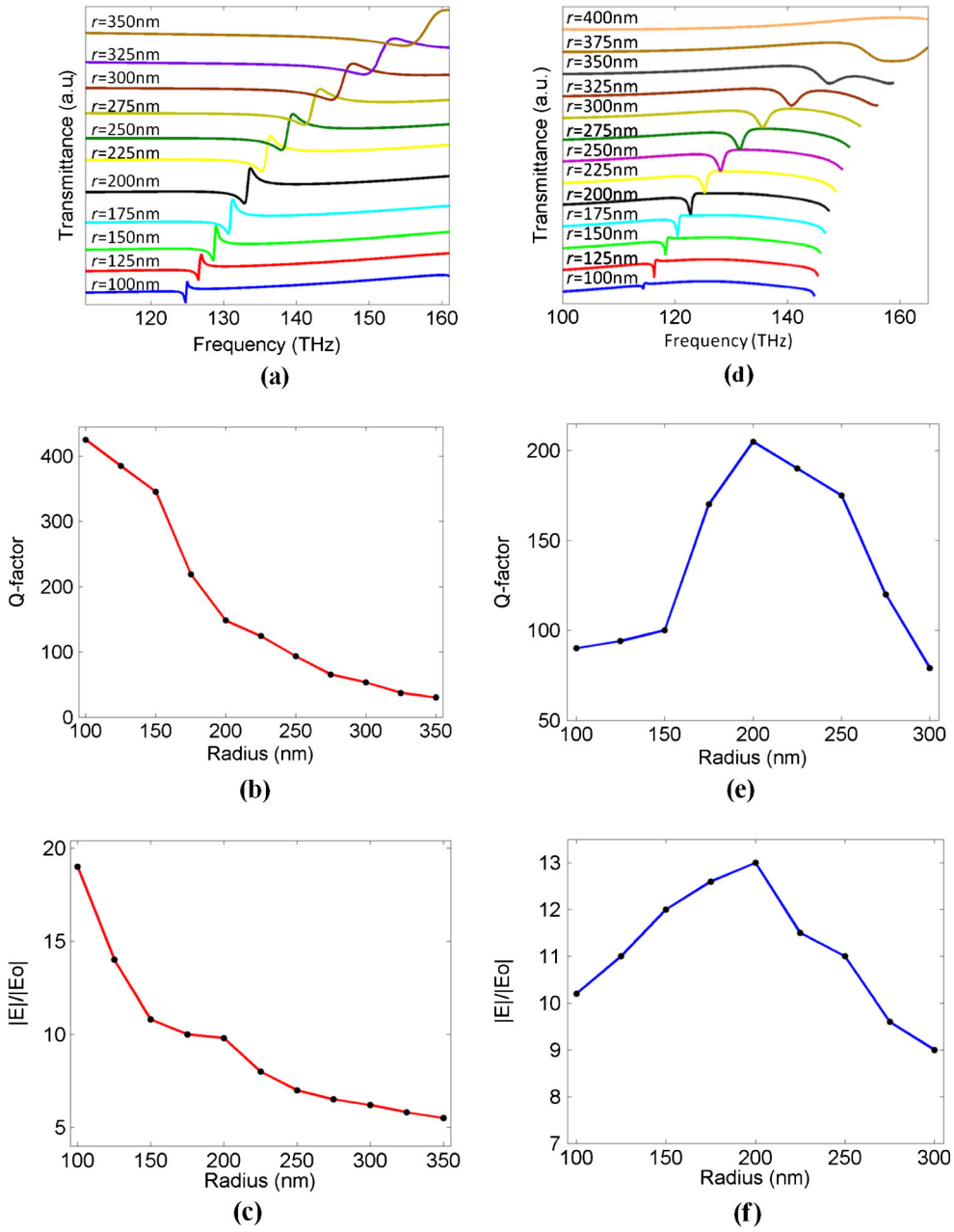

Fig. 3 **a** Transmittance spectra for different values of r at fix t=250 nm. **b** Extracted Q-factor as a function of r. **c** Electric field enhancement at different r values. **d** Transmittance spectra for different values of r at fix t= 350 nm. **e** Extracted Q-factor as a function of r. **f** Electric field enhancement at different r values

which make it a better choice for slow-light devices. The electric field enhancement is also calculated at different values of t as shown in Fig. 2c. The enhancement increases with the increase in t values, which means that more energy will be localized in the cavity for large values of t. However, for t values above than 400 nm, the field enhancement somewhat remains the same. The maximum value of the field enhancement achieved is above 13.

We next analyzed the EIT and Fano resonances by fixing the thickness t and changing the radius r of the cylindrical hole. Since in the above calculations, at t=250 nm, sharp asymmetric Fano line shape, and at t=350 nm, sharp EIT dip are observed. Therefore, we choose two values of t and analyzed the transmittance spectra. Figure 3a shows the transmittance characteristics for different values of r at fixed t= 250 nm. A large blue-shift of the Fano resonant mode is observed by increasing the values of r from 100 to 350 nm. The line shape of the Fano resonance also changes with great amount because the cavity modes and solid silicon block modes mixes highly as we modify the radius. Figure 3b illustrates the Q-factor for various values of r. It appears that the Q-factor decreases as we increase r. This is because that by increasing r, the effective size of the block decreases, which decrease the near-field coupling, leads to low Q-factor. In this case, the highest value of Q-factor achieved is 425 for r= 100 nm, which is highly suitable for slow-light devices. Figure 3c shows the electric field enhancement spectra versus r. As we increase r, the field enhancement gradually decreases and a very small amount of energy is localized for higher values of r. The maximum enhancement value achieved is 19 at r=100 nm.

Table 1 Q and NFE values calculated at EIT and Fano resonances for different values of Δx

Δx	100 nm	150 nm	200 nm
F_1	$Q\approx442$	$Q\approx442$	$Q\approx266$
	NFE≈13	NFE≈30	NFE≈36
F_2	$Q\approx432$	$Q\approx256$	$Q\approx635$
	NFE≈2	NFE≈2	NFE≈1
EIT_1	$Q\approx597$	$Q\approx394$	$Q\approx584$
	NFE≈25	NFE≈26	NFE≈33
EIT_2	$Q\approx377$	$Q\approx284$	$Q\approx162$
	NFE≈7	NFE≈5	NFE≈4

Figure 3d reveals the transmittance characteristics of SHB nanostructure for various values of r at fix t=350 nm. The EIT resonances show a large blue shift in the spectrum by varying r. The dip of the EIT resonances grows, and the spectral width broadened as we increase r. However, for large values of r (350 to 400 nm), the hybridized modes couple weakly because the actual size of the silicon block reduces due to which the EIT resonance completely vanishes. Figure 3e shows the calculated Q-factors against the r values. The Q-factor increases gradually by changing r from 100 to 200 nm. However, by further increasing the r values, the Q-factor severely drops similar like in Fig. 3b. Figure 3f illustrates the electric field enhancement as a function of radius. The enhancement

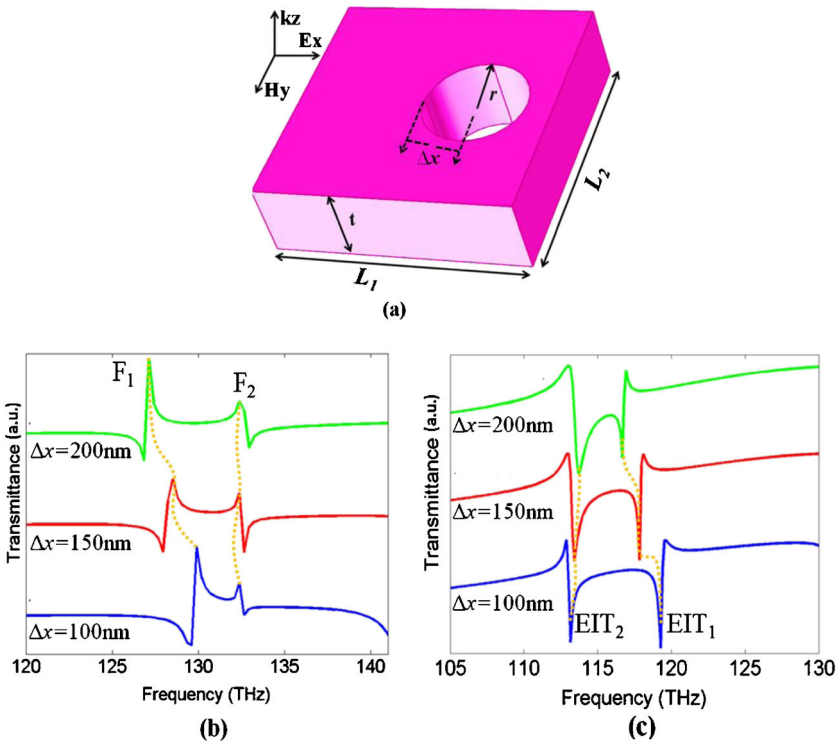

Fig. 4 **a** Schematic of asymmetric SHB nanostructure. Transmittance spectra of asymmetric SHB at **b** t=250 nm and **c** t=350 nm

increases in the beginning and then declines by increasing r. The highest value of the field enhancement observed is 13 for r=200 nm.

Breaking Symmetry

Eventually, we introduce the symmetry breaking conception in SHB by displacing the cylindrical hole in the x-direction similar like plasmonic nanostructures [10, 11, 13, 27]. The reduction in symmetry enables the higher-order hybridized modes to interact with each other. Due to this, new higher-order hybridized modes will appear in the spectrum similar like plasmonic nanosystems [10, 11, 13, 27]. So, we considered the SHB nanostructure shown in Fig. 4a. The parameter Δx denotes the displacement of the cavity from center position. First, we calculated the transmittance characteristics shown in Fig. 4b of SHB nanostructure with the following parameters: L_1=L_2=1000 nm, t=250 nm, and r=200 nm, respectively. The transmittance spectra are obtained for three different values of Δx, i.e., 100, 150, and 200 nm. At Δx= 100 nm (blue curve), a new higher-order hybridized mode as expected appear on the high energy shoulder of the first Fano resonance (F_1), which overlaps the broad dipole mode and induces a sharp asymmetric Fano line shape (F_2) near 132 THz. This mode was dark in the concentric case. The line shape of F_2 is found opposite to that of F_1 and remains at the same spectral position by increasing the value of Δx. However, the first Fano resonance F_1 is highly red-shifted as we increase Δx. The similar higher order modes are reported in metal nanostructures, which suffers from large ohmic losses [27, 29, 36]. Thus, dual Fano resonances with sharp asymmetric line shapes are achieved in SHB nanostructure, which in our knowledge has never been seen in any dielectric nanostructure reported before [31, 33–35]. With the increase in the value of Δx, the amplitude of the second Fano resonance F_2 matures and the spectral gap between the two Fano resonances increases due to strong modes interaction. The calculated Q-factors (Q) and maximum near-field enhancement (NFE) values at each Fano resonance are shown in Table 1. Extremely high Q and NFE values are observed with almost unity transmission, which are greatly suitable for low loss slow-light devices and multi-wavelength biosensing applications.

Figure 4c demonstrates the transmittance spectra of asymmetric SHB calculated for t= 350 nm. In this case, the similar higher-order hybridized mode is observed near 113 THz (blue curve) by breaking the symmetry of the structure. The new excited mode interacts with the bright dipolar mode and engenders the second EIT resonance (EIT_2). Here, EIT_2 appears at the lower energy shoulder of the first EIT resonance (EIT_1). This situation is different from the previous case, where the higher-order mode emerged at the high energy shoulder of the first Fano resonance. Furthermore, by increasing Δx, the line shape of both the EIT resonances transform into sharp asymmetric Fano line shapes and the spectral gap between them slightly reduces. Thus, by breaking the symmetry of the structure, the EIT resonances translated to Fano resonances. The Q and NFE values calculated at both the EIT resonances are presented in Table 1, where the highest Q achieved is 584 with NFE=33, which is highly appropriate for low loss slow-light devices and multi-wavelength biosensors.

Conclusion

We proposed a simple planar silicon holey block, which exhibits EIT and Fano resonances by properly adjusting the geometrical parameters. These resonances emerge due near-field coupling between the solid block modes and cavity modes. The line shape of both the EIT and Fano resonances can be modified and tuned by changing different parameters of the SHB nanostructure. The symmetry of the structure is also broken and dual EIT and Fano resonances are obtained in the transmittance spectrum. To our knowledge, such multiple resonances supported by our design have never been reported before in any dielectric nanostructure. Furthermore, the large field enhancement and extremely high Q-factors calculated at each EIT and Fano resonances provide an effective platform for low loss slow-light devices and multi-wavelength biosensing applications.

References

1. Harris SE (2008) Electromagnetically induced transparency. Phys Today 50(7):36–42
2. Zhang S, Genov DA, Wang Y, Liu M, Zhang X (2008) Plasmon-induced transparency in metamaterials. Phys Rev Lett 101(4): 47401
3. Liu N, Langguth L, Weiss T, Kästel J, Fleischhauer M, Pfau T, Giessen H (2009) Plasmonic analogue of electromagnetically induced transparency at the Drude damping limit. Nat Mater 8(9): 758–762
4. Lu Y, Jin X, Zheng H, Lee Y, Rhee JY, Jang WH (2010) Plasmonic electromagnetically-induced transparency in symmetric structures. Opt Express 18(13):13396–13401
5. Chai Z, Hu X, Zhu Y, Zhang F, Yang H, Gong Q (2013) Low-power and ultrafast all-optical tunable plasmon-induced transparency in plasmonic nanostructures. Appl Phys Lett 102(20):201119
6. Liu H, Li B, Zheng L, Xu C, Zhang G, Wu X, Xiang N (2013) Multispectral plasmon-induced transparency in triangle and nanorod (s) hybrid nanostructures. Opt Lett 38(6):977–979
7. Amin M, Farhat M, Bağcı H (2013) An ultra-broadband multilayered graphene absorber. Opt Express 21(24):29938–29948
8. Amin M, Bağci H (2012) Investigation of Fano resonances induced by higher order plasmon modes on a circular nano-disk with an elongated cavity. Prog Electromagn Res 130:187–206

9. Khan AD, Amin M, Iqbal MY, Ali A, Khan R, Khan SD (2015) Twin dipole Fano resonances in symmetric three-layered plasmonic nanocylinder. Plasmonics 1–8
10. Khan AD, Miano G (2013) Higher order tunable Fano resonances in multilayer nanocones. Plasmonics 8(2):1023–1034
11. Khan AD, Miano G (2013) Plasmonic Fano resonances in single-layer gold conical nanoshells. Plasmonics 8(3):1429–1437
12. Khan AD, Miano G (2013) Investigation of plasmonic resonances in mismatched gold nanocone dimers. Plasmonics 9(1):35–45
13. Khan AD, Khan SD, Khan RU, Ahmad N (2014) Excitation of multiple Fano-like resonances induced by higher order plasmon modes in three-layered bimetallic nanoshell dimer. Plasmonics 9(2):461–475
14. Khan AD, Khan SD, Khan R, Ahmad N, Ali A, Khalil A, Khan FA (2014) Generation of multiple Fano resonances in plasmonic split nanoring dimer. Plasmonics 9(5):1091–1102
15. Khan A, Miano G (2011) Fano resonance by symmetry breaking in silver-silica-gold multilayer nanoshells. In: High Capacity Optical Networks and Enabling Technologies (HONET), IEEE, pp 233–236
16. Khan AD (2014) Multiple Fano resonances in bimetallic layered nanostructures. Int Nano Lett 4(2):1–12
17. Chen J, Wang P, Chen C, Lu Y, Ming H, Zhan Q (2011) Plasmonic EIT-like switching in bright-dark-bright plasmon resonators. Opt Express 19(7):5970–5978
18. Sun Y, Tong Y-W, Xue C-H, Ding Y-Q, Y-h L, Jiang H, Chen H (2013) Electromagnetic diode based on nonlinear electromagnetically induced transparency in metamaterials. Appl Phys Lett 103(9):091904
19. Rahmani M, Luk'yanchuk B, Hong M (2013) Fano resonance in novel plasmonic nanostructures. Laser Photonics Rev 7(3):329–349
20. Fang Z, Cai J, Yan Z, Nordlander P, Halas NJ, Zhu X (2011) Removing a wedge from a metallic nanodisk reveals a Fano resonance. Nano Lett 11(10):4475–4479
21. Peña-Rodríguez O, Rivera A, Campoy-Quiles M, Pal U (2013) Tunable Fano resonance in symmetric multilayered gold nanoshells. Nanoscale 5(1):209–216
22. Yang Z-J, Zhang Z-S, Zhang L-H, Li Q-Q, Hao Z-H, Wang Q-Q (2011) Fano resonances in dipole-quadrupole plasmon coupling nanorod dimers. Opt Lett 36(9):1542–1544
23. Biswas S, Duan J, Nepal D, Park K, Pachter R, Vaia RA (2013) Plasmon-induced transparency in the visible region via self-assembled gold nanorod heterodimers. Nano Lett 13(12):6287–6291
24. Mei Z, Liang-Sheng L, Ning Z, Qing-Fan S (2013) The Fano-like resonance in self-assembled trimer clusters. Chin Phys Lett 30(7):077802
25. Mirin NA, Bao K, Nordlander P (2009) Fano resonances in plasmonic nanoparticle aggregates†. J Phys Chem A 113(16):4028–4034
26. Liu S-D, Yang Z, Liu R-P, Li X-Y (2012) Multiple Fano resonances in plasmonic heptamer clusters composed of split nanorings. ACS Nano 6(7):6260–6271
27. Mukherjee S, Sobhani H, Lassiter JB, Bardhan R, Nordlander P, Halas NJ (2010) Fanoshells: nanoparticles with built-in Fano resonances. Nano Lett 10(7):2694–2701
28. Hao F, Sonnefraud Y, Dorpe PV, Maier SA, Halas NJ, Nordlander P (2008) Symmetry breaking in plasmonic nanocavities: subradiant LSPR sensing and a tunable Fano resonance. Nano Lett 8(11):3983–3988
29. Liu S-D, Yang Y-B, Chen Z-H, Wang W-J, Fei H-M, Zhang M-J, Wang Y-C (2013) Excitation of multiple Fano resonances in plasmonic clusters with D2h point group symmetry. J Phys Chem C 117(27):14218–14228
30. Miroshnichenko AE, Kivshar YS (2012) Fano resonances in all-dielectric oligomers. Nano Lett 12(12):6459–6463
31. Chong KE, Hopkins B, Staude I, Miroshnichenko AE, Dominguez J, Decker M, Neshev DN, Brener I, Kivshar YS (2014) Observation of Fano resonances in all-dielectric nanoparticle oligomers. Small 10(10):1985–1990
32. Filonov DS, Slobozhanyuk AP, Krasnok AE, Belov PA, Nenasheva EA, Hopkins B, Miroshnichenko AE, Kivshar YS (2014) Near-field mapping of Fano resonances in all-dielectric oligomers. Appl Phys Lett 104(2):021104
33. Pu M, Song M, Yu H, Hu C, Wang M, Wu X, Luo J, Zhang Z, Luo X (2014) Fano resonance induced by mode coupling in all-dielectric nanorod array. Appl Phys Express 7(3):032002
34. Yang Y, Kravchenko II, Briggs DP, Valentine J (2014) All-dielectric metasurface analogue of electromagnetically induced transparency. Nat Commun 5
35. Zhang J, Liu W, Zhu Z, Yuan X, Qin S (2014) Strong field enhancement and light-matter interactions with all-dielectric metamaterials based on split bar resonators. Opt Express 22(25):30889–30898
36. Li J, Liu T, Zheng H, Dong J, He E, Gao W, Han Q, Wang C, Wu Y (2014) Higher order Fano resonances and electric field enhancements in disk-ring plasmonic nanostructures with double symmetry breaking. Plasmonics 9(6):1439–1445